

## Validation of a numerical model of locally cooled tissues

Piotr Buliński, Ziemowit Ostrowski, Wojciech Adamczyk,  
Artur Fityka, Andrzej J. Nowak  
*Institute of Thermal Technology*  
*Silesian University of Technology*  
*Konarskiego 22, 44-100 Gliwice, Poland*  
*e-mail: ziemowit.ostrowski@polsl.pl*

Measurements of heat transfer and temporal temperature distribution can be used as input in the diagnostic tools and methods of skin lesions, with special attention paid to malignant melanoma identification. Such approach requires mutual use of skin temperature and heat flux measurements combined with numerical simulation. A mild skin cooling process by a brass compress is considered in this paper. The temperature distribution on the skin and the heat flux between metal and tissues are measured. They are used in the course of validation study of the proposed numerical model. A numerical model of heat transfer in living tissues is described by Pennes' bioheat equation augmented with additional models of passive thermoregulation and vasoconstriction effects. The information regarding material properties of tissues and cooling compress involved in the simulation is essential to accurately solve this problem. Therefore, the main purpose of this work is to determine the accurate material property information by means of laboratory experiments.

**Keywords:** bioheat transfer, LFA, melanoma, thermal conductivity, thermal diffusivity.

### NOMENCLATURE

- $a_{cs}$  – distribution factor for vasoconstriction [-],
- $c$  – specific heat [ $\text{J}\cdot\text{kg}^{-1}\cdot\text{K}^{-1}$ ],
- $C_s$  – vasoconstriction signal [-],
- $k$  – thermal conductivity [ $\text{W}\cdot\text{m}^{-1}\cdot\text{K}^{-1}$ ],
- $q$  – heat production rate [ $\text{W}\cdot\text{m}^{-3}$ ],
- $\mathbf{r}$  – vector coordinate [m],
- $T$  – temperature [K],
- $t$  – time [s],
- $\beta$  – blood perfusion energy equivalent [ $\text{W}\cdot\text{m}^{-3}\cdot\text{K}^{-1}$ ],
- $\mu$  – empirically estimated proportionality constant [ $\text{K}^{-1}$ ],
- $\rho$  – density [ $\text{kg}\cdot\text{m}^{-3}$ ],
- $\omega$  – perfusion [ $\text{s}^{-1}$ ].

### SUBSCRIPTS

- a – artery,
- b – blood,
- m – metabolic,
- p – perfusion,
- 0 – thermoneutral conditions.

## 1. INTRODUCTION

The accurate numerical models of living tissue can play a critical role in modern biomedical engineering. Such models can allow to understand processes taking place in a living tissue itself as well as they can help to develop a new treatment and/or equipment used to assist medical staff during diagnosis and controlled treatment process [11]. The work presented here is a part of wider research/project targeted at investigating the possibility of early diagnosis of skin lesions, with special attention paid to identification of an early stage of malignant melanoma. However, numerical simulations are not the only aim of this project. Measurements of heat transfer and temporal temperature distribution can also be used as input in diagnostic tools and methods of skin lesions.

In the previous work of this research team [5], the thermographic (infrared- IR camera) measurements of skin recovering from local cooling were used to validate the numerical model. However, during the above mentioned research, additional model validation possibilities were identified. The follow up research was targeted at model validation employing skin – cooling compress interfacial heat flux measurements [6]. In a new experimental set-up, including a custom designed cuboid brass cooling compress, the measuring and recording of the transferred heat flux using differential thermopile sensor was proposed. Comparison of the numerical model response with experimental data showed that the model roughly ‘meets’ the *in vivo* measurements, which means that the simplified model of bioheat transfer with only/just passive thermoregulation is not sufficient to describe complex cooling and recovery process of human tissues.

The main purpose of this study is to examine the material measurements of brass compress which was employed for *in vivo* experiment. Thanks to laser flash analysis (LFA) it is possible to accurately examine the compress heat conductivity, and the properly prepared sample gives the information about the compress density. In addition, the numerical model is developed including a vasoconstriction model. Vasoconstriction is a process of narrowing of the blood vessels caused by the contraction of the smooth muscle of blood vessel wall. Therefore, less heat is introduced to the tissue by means of blood perfusion. Generally, the implemented model provides additional thermal resistance in reference to local temperature. Finally, the simulation is validated against data from the skin cooling experiment conducted on small group of subjects, in which heat flux and temperature of compress over time are measured over time.

## 2. MATHEMATICAL MODEL

The passive part of heat transfer in the living tissues is described by Pennes’ bioheat equation [7]:

$$c\rho\frac{\partial T(\mathbf{r},t)}{\partial t} = \nabla [k(T)\nabla T(\mathbf{r},t)] + q_m(\mathbf{r},t) + \omega_b(\mathbf{r},t)c_b\rho_b[T_a - T(\mathbf{r},t)], \quad (1)$$

where  $c$ ,  $c_b$  – specific heat (tissue and blood, respectively),  $\rho$ ,  $\rho_b$  – density (tissue and blood, respectively),  $T$ ,  $T_a$  – temperature (tissue and perfusing (artery) blood, respectively),  $t$  – time,  $k$  – the tissue heat conductivity,  $q_m$  – the metabolic heat production rate,  $\omega_b$  – the blood perfusion rate, and  $\mathbf{r}$  – the vector coordinate.

The metabolic heat production rate  $q_m$  is the sum of the basal value  $q_{m,0}$  and the additional  $\Delta q_m$  part, being a result of autonomic thermoregulation:

$$q_m = q_{m,0} + \Delta q_m, \quad (2)$$

where  $q_{m,0}$  is the metabolic heat production rate for thermoneutral conditions (i.e., body in thermal equilibrium with environment).

Under non-neutral conditions, metabolic rates vary with the local tissue temperature. The influence of temperature on metabolism is modelled according to the  $Q_{10}$  relation which states that

for every 10 K reduction (change) in the tissue temperature, there is a corresponding reduction (change) in the cell metabolism  $\Delta q_m$  by the factor  $Q_{10} = 2$ , as reported in [1]:

$$\Delta q_m = q_{m,0} \cdot \left[ 2^{(T-T_0)/10} - 1 \right], \quad (3)$$

where  $T_0$  is the basal temperature distribution (i.e., in thermoneutral conditions).

In non-neutral conditions, the perfusion rate  $\omega_b$  (i.e., the tissue blood flow related to tissue value) varies with changes in regional metabolic rates as well. The dependency of the perfusion rate  $\omega_b$  change on variations of the metabolic heat production rate  $\Delta q_m$  (3) is linear [8, 9]:

$$\Delta\beta = \mu_b \Delta q_m, \quad (4)$$

where  $\beta = \omega_b c_b \rho_b$  – blood perfusion energy equivalent, while  $\mu_b = 0.932 \text{ K}^{-1}$  – empirically estimated proportionality constant [1, 10].

Using the above definition of  $\beta$ , the last term on the right of Eq. (1), which is a source term arising from the arterial blood perfusing the tissue, reads:

$$q_p = \beta(T_a - T) = (\beta_0 + \Delta\beta)(T_a - T) = (\omega_{b,0} c_b \rho_b + \mu_b \Delta q_m)(T_a - T), \quad (5)$$

where  $\omega_{b,0}$  is the basal perfusion rate for thermoneutral conditions.

In this study, the active part of thermoregulation was employed by means of vasoconstriction. Vasoconstriction was applied to skin and muscle, while for fat layer only passive thermoregulation was used (Eq. (5)). According to Stolwijk's [10] the vasoconstriction formulation can be described by  $Q_{10}$  relationship:

$$\frac{\beta}{\beta_0} = \frac{1}{1 + a_{cs,i} C_s} \cdot 2^{(T-T_0)/10}, \quad (6)$$

where  $a_{cs,i}$  is the distribution factor for vasoconstriction, and  $C_s = 0.0695$  – vasoconstriction signal.

The value of distribution factor for vasoconstriction is based on Fiala [2] and for the arm it is equal to 0.1945. Neither shivering thermogenesis nor sweating was introduced in the model at hand. The final form of perfusion part of bioheat transfer equation source term for skin and muscle layers is as follows:

$$q_p = \beta(T_a - T) = \left( \beta_0 \cdot \frac{1}{1 + a_{cs,i} C_s} \cdot 2^{(T-T_0)/10} \right) (T_a - T). \quad (7)$$

The numerical model of human forearm, cooling compress and their surrounding was developed. The numerical simulations were carried out using the ANSYS FLUENT 14 commercial computational fluid dynamics (CFD) package (ANSYS Inc., USA). The additional source terms of heat conduction equation arising in bioheat transfer Eq. (1) were introduced by means of user-defined function (UDF) in the ANSYS FLUENT code. The 3D geometrical model of the computational domain is presented in Fig. 1. The human forearm was modelled as a cylinder. Multiple concentric homogeneous layers representing different tissues types (bone, muscle, fat, inner skin, and outer skin) were considered. The outer diameter of each layer is shown in Table 1. The modelled length of the arm was 200 mm which is enough to provide the solution of independence of the boundary condition applied on the external boundaries – thermal insulation. Due to the symmetry of the model, only a quarter of the model was considered. A small cylindrical volume on top of the forearm represents the cooling compress used in the thermal stimulation (cooling) of skin. To simplify the geometry and to facilitate the discretization of numerical domain, the deformation of tissue under the compress pressure was neglected. Contrary to reality, the tissue is non-deformable while the compress is rounded in order to provide contact over the entire surface.

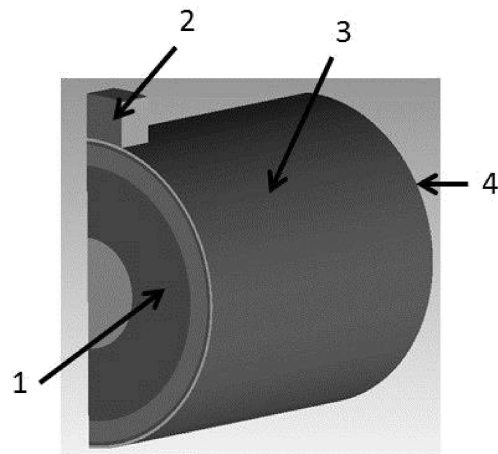


**Fig. 1.** 3D geometrical model of computational domain: 1 – tissues layers: bone, muscle, fat, inner skin, and outer skin, 2 – cooling compress, 3 – forehand outer skin, 4 – insulated wall: back & front.

**Table 1.** Dimensions and properties of tissues and initial values of model variables (for steady-state analysis).

Tissue	Outer radius [mm]	Thermal cond. [ $\text{W}\cdot\text{m}^{-1}\cdot\text{K}^{-1}$ ]	Density [ $\text{kg}\cdot\text{m}^{-3}$ ]	Specific heat [ $\text{J}\cdot\text{kg}^{-1}\cdot\text{K}^{-1}$ ]	Perfusion rate [ $\text{s}^{-1}$ ]	Metabolic heat production rate [ $\text{W}\cdot\text{m}^{-3}$ ]
Outer skin	42.9	0.47	1085	3680	0	0
Inner skin	42.1	0.47	1085	3680	0.0011	631
Fat	41.1	0.16	850	2300	0.0000036	58
Muscle	35.3	0.42	1085	3768	0.000538	684
Bone	15.3	0.75	1357	1700	0	0

The numerical mesh was generated using ICEM CFD (ANSYS Inc., USA). A blocking scheme was applied in order to provide high-quality hexahedral mesh. The grid was refined in the areas where high temperature gradients are expected (especially in the skin layers under the compress). The final mesh is presented in Fig. 3, it contains 1.4 M elements. To improve its quality, every element was smoothed with the appropriate tool in the used software. To check the quality of the grid, the aspect ratio was tested (i.e., scaled ratio between the volume of the element and the radius of its circumscribed sphere to the power of three). The mesh quality histogram is presented in Fig. 2, where 0 corresponds with the worst elements and 1 relates to the best elements. All elements have a quality above 0.8, which means the mesh is of high quality.

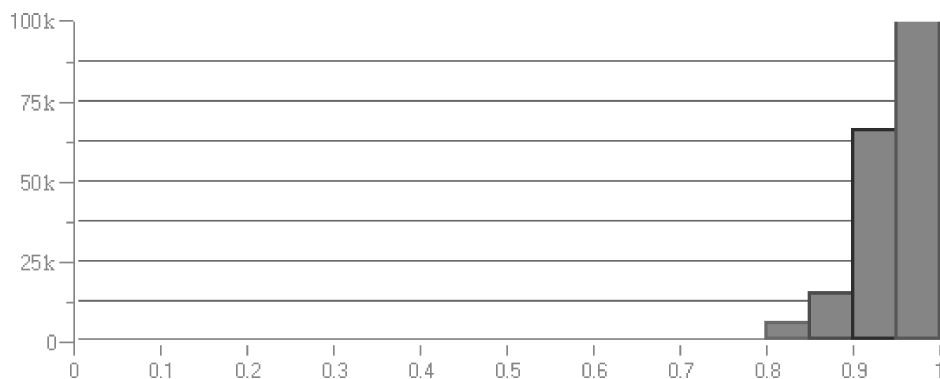


**Fig. 2.** Histogram of quality of numerical partition elements; 1 – the best, 0 – the worst.

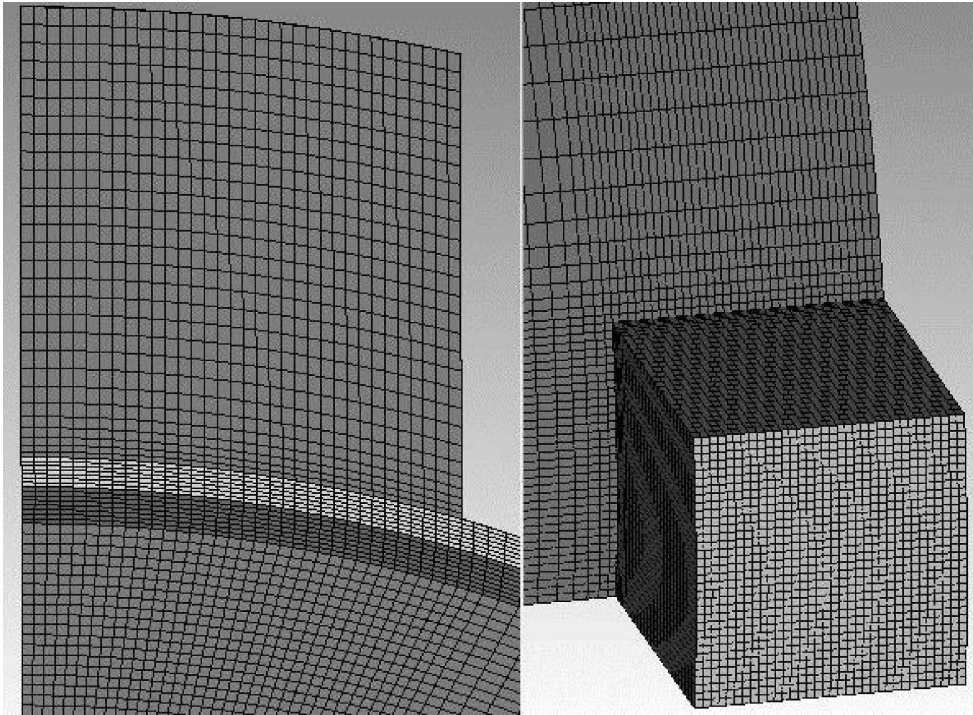


**Fig. 3.** Selected regions of numerical mesh: in symmetry plane (left) and seen from above the compress (right).

The final model was composed of one differential equation. The second-order upwind scheme was applied to solve it. According to the sensitivity analysis of different time discretization schemes [5] three time steps were selected and tested against their influence on the results, namely: 0.25 s, 0.5 s and 1 s. Taking into account the obtained results and the computation time, the time step of 0.5 s was selected for transient simulation in the current study. The material properties of every simulated human tissue are presented in Table 1. Heat was applied only to three layers: inner skin, fat and muscle. The material properties of these three tissue types, hard to measure *in vivo*, are based on the well-established literature sources [1]. In the experimental part of this study, the material properties of brass compress were measured. Brass compress density was measured by means of direct method and its thermal diffusivity was examined using laser flash analysis (LFA). Density of brass was set to  $8500 \text{ kg/m}^3$ , thermal conductivity to  $101 \text{ W/(m}\cdot\text{K)}$  and specific heat to  $380 \text{ J/(kg}\cdot\text{K)}$ .

### 3. EXPERIMENT

The information regarding the material properties of tissues and cooling compress involved in the simulation is essential to accurately solve this problem. The sensitivity analysis based on the results obtained in previous simulations shows that thermal properties of cooling compress (i.e., its specific heat capacity, heat diffusivity and density) are of high importance. Therefore, the main purpose of this work is to determine the accurate material property information by means of laboratory experiments. The numerical results with precise properties are then validated against measurement data.

An LFA is employed to determine the diffusivity of compress. In this method, the sample of material is exposed to laser pulse. The front surface of sample is heated up. Due to conduction, the temperature of the backside metal surface increases. The temperature difference in time between both sides is proportional to heat diffusivity [4]. Heat capacity is examined by using differential scanning calorimetry (DSC). The objective of the DSC operation is to measure the excessive heat

supplied to the investigated sample material compared to the reference sample which undergoes the same temperature process. Since the heat recorded by DSC is proportional to the sample heat capacity, such measurements can be used to determine the heat capacity of the sample [3]. The value of heat capacity can be calculated as the following equation:

$$\Delta T(L, S) = \frac{Q}{\rho \cdot c \cdot L \cdot \frac{\pi^2 \cdot S}{4}} \cdot \left[ \sum_{n=1}^{\infty} (-1)^n \cdot \exp\left(-\frac{n^2 \cdot \pi^2 \cdot \alpha \cdot t}{L^2}\right) \right], \quad (8)$$

where  $L$  is the height of the sample [m],  $S$  – the width (diameter) of the sample [m],  $Q$  – the heat absorbed by the sample [J],  $\rho$  – the density of the sample material [ $\text{kg}\cdot\text{m}^{-3}$ ],  $c$  – the specific heat capacity [ $\text{J}\cdot(\text{kg}\cdot\text{K})^{-1}$ ],  $\alpha$  – the thermal diffusivity [ $\text{mm}^2\cdot\text{s}^{-1}$ ], and  $t$  – time [s].

The results of thermal diffusivity measurement and derived thermal conductivities are shown in Table 2. These results are compared against the values of thermal conductivity previously used in the numerical simulations and obtained from the literature. The mathematical model is very sensitive to introduced coefficients of values as it was mentioned. For this reason, the incorrectly adopted density and conductivity can cause discrepancies between the simulation results and data collected during the research.

**Table 2.** Results of measurement *versus* previously used values.

	Thermal diffusivity [ $\text{mm}^2\cdot\text{s}^{-1}$ ]	Measured thermal conductivity [ $\text{W}\cdot\text{m}^{-1}\cdot\text{K}^{-1}$ ]	Literature data thermal conductivity [ $\text{W}\cdot\text{m}^{-1}\cdot\text{K}^{-1}$ ]	Relative error [%]
Compress alloy	34.5	101	110	8

To examine the accuracy of numerical model, the *in vivo* measurements were carried out. The experiment was approved by the Medical Ethical Committee of the Maria Skłodowska-Curie Memorial Cancer and Institute of Oncology Gliwice Branch. Each subject of the study gave a written consent prior to participation in this study. For the analysis at hand, the group of four adult males was selected. The subjects' characteristics (mean  $\pm$  SD) are: age  $30.8 \pm 5.4$ , height  $1.83 \pm 0.07$  m, weight  $98.5 \pm 16.5$  kg. The studied skin sites were dorsal and ventral side of the left forearm halfway the wrist and inner side of the elbow, resulting in  $N = 8$  samples. The subjects were asked to stay in sited for 15 minutes prior to the measurements. Subjects' skin was cooled by the brass compress at stabilized initial temperature of  $7(8)^\circ\text{C}$  by means of thermoelectric cooling device (in house design). In order to prevent the experiment from being disturbed by external heat sources (sinks), the cooling compress was isolated by extruded polystyrene foam. The compress covered (side and top) with expanded polystyrene (EPS) block was first placed on a cooling device. Once a stable and uniform temperature of the brass compress was reached, the compress together with EPS insulation was placed on the subjects' forearm skin. The temperatures of compress (center – mid and top plane) and heat flux were then recorded for 15 seconds.

The temperature of the brass compress (at mid and top plane) was measured using calibrated T-type thermocouples of diameter 0.5 mm (CZAKI THERMO-PRODUCT, Poland). The Micro-Foil<sup>®</sup> (RdF Corp., USA) Model 27160 Heat Flux Sensor was used to measure the heat flux on the brass compress/skin interface. This sensor is a differential thermopile. Heat passing through a calibrated polyimide membrane produces a small temperature difference. The signal is proportional to the difference in temperature and the number of junctions in the thermopile. Because the active sensor area is  $12 \times 24$  mm, the set of two heat flux sensors was used to cover the whole skin/compress interfacial area. All the data were acquired and recorded using a personal computer (PC) running LabView Signal Express<sup>®</sup> software and 24-Bit Universal Analog Input cards, type NI9214 (National Instruments, USA).

#### 4. NUMERICAL RESULTS

Numerical computations were carried in two steps:

- steady-state simulation of thermoneutral conditions being initial state for the following step,
- transient simulation of skin cooling.

Steady-state simulation was performed in order to get an initial temperature distribution and to tune model variables: the metabolic heat production rate  $q_m$  and the perfusion rate  $\omega_b$  as in the thermoneutral state (i.e., in the model in thermal equilibrium with environment). During this step, type of volume representing cooling compress was turned off. On the outer skin, the convection boundary conditions with convective heat transfer coefficient of  $5 \text{ W}/(\text{m}^2 \cdot \text{K})$  and air temperature of  $23^\circ\text{C}$  were specified. Tissue properties, initial metabolic heat production rates and perfusion rates used in steady-state calculations are presented in Table 1 after [8, 9]. The temperature distribution being the result of steady-state analysis (shown in Figs. 4 and 5) is then prescribed as an initial

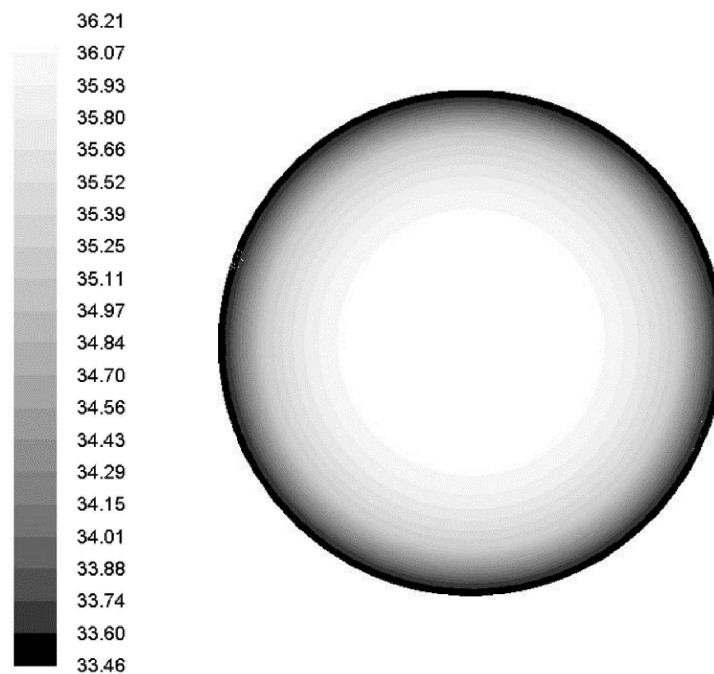


Fig. 4. Initial tissue temperature (in  $^\circ\text{C}$ ) distribution (in symmetry plane) for transient analysis.

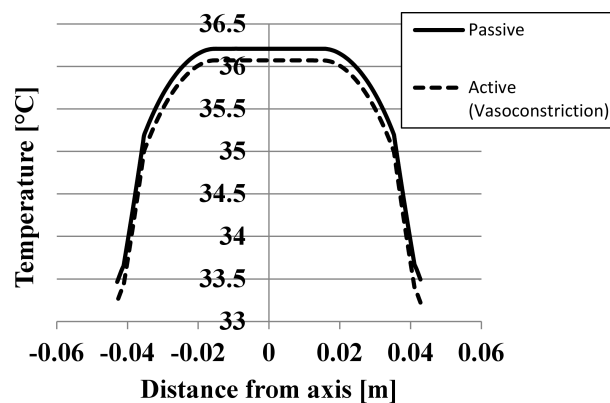


Fig. 5. Initial tissue temperature ( $^\circ\text{C}$ ) distribution (in axis) for transient analysis for two types of thermoregulation: passive (solid line) and active (dashed line).

condition for further transient calculations. In addition, the resulting distributions of temperature, metabolic heat production rate and perfusion rate are thereafter treated as

- basal temperature distribution  $T_0$ ,
- basal metabolic heat production rate  $q_{m,0}$ , and
- basal blood perfusion rate  $\omega_{b,0}$ ,

included in Eqs. (2), (3), (5) and (7).

In the skin layer, the temperature difference between the passive and the active thermoregulation model is equal to  $0.3^\circ\text{C}$ . This means that the vasoconstriction model provides a better insulation of inner tissues. In addition, the bone and muscle temperature is lower for active thermoregulation. This is caused by new perfusion source term which was used for the muscle. It generates less heat by means of perfusion.

Transient computations were then conducted to mimic the skin and compress cooling procedure, the material type of volume representing cooling compress was turned on and switched to solid with the measured properties of brass compress and the prescribed uniform initial temperature of  $8^\circ\text{C}$ . For this step, the skin surface and the outer surface of compress were insulated (as the compress was covered with thermal insulation block). Then, transient simulation began to mimic 15 s of local skin cooling. As a first attempt, ideal contact between the cooling compress and the skin was assumed in the model at hand. However, the simulated heat fluxes and the compress temperature response were far from those measured as reported in [5]. The origin of such behavior is identified (among others) as being a result of:

- the presence of hairs,
- limited allowable cooling compress pressure on skin,
- additional contact resistance introduced by MicroFoil<sup>®</sup> heat flux sensor itself.

To simulate non-ideal contact conditions taking place during the experiment, the contact resistance of  $0.00025 \text{ m}^2\cdot\text{K}\cdot\text{W}^{-1}$  was implemented in the numerical model (on the skin-compress interface). The tissue and compress temperature distribution (in symmetry plane) for 15 s of simulation are shown in Fig. 6. Figure 7 shows the CFD simulation result compared to the mean  $\pm\text{SD}$

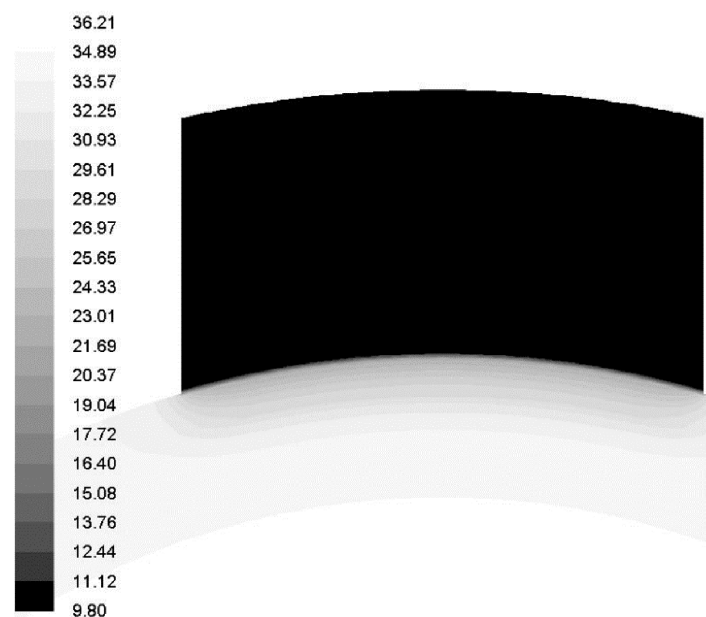


**Fig. 6.** Tissue and compress temperature distribution (in symmetry plane) for 15 s of simulation.

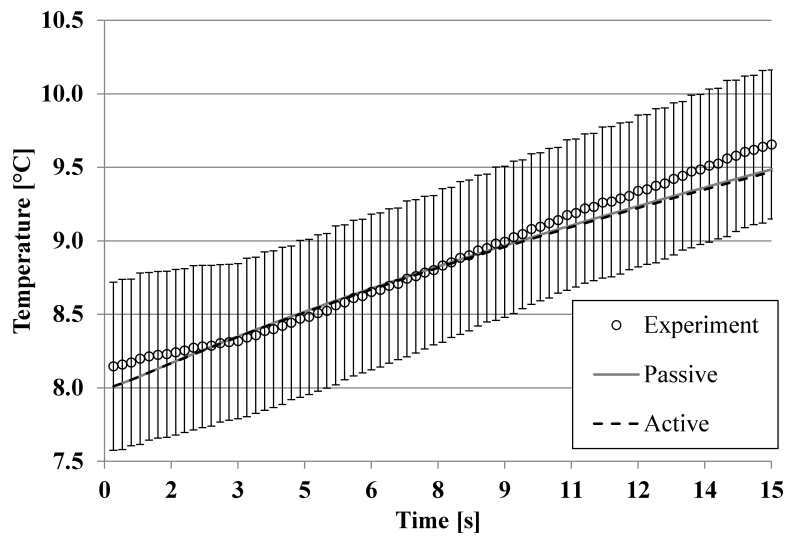


**Fig. 7.** Compress center mid-plane temperature ( $^{\circ}\text{C}$ ) vs. time (s) for experiment (mean  $\pm$ SD,  $N = 8$  samples) and CFD simulation for both passive and active thermoregulation models.

of  $N = 8$  recorded compress temperature history samples (the compress temperature at the center mid-plane point). The penetration of low temperature inside the tissue is shallow. After 15 s of cooling, the outer and inner skin temperature decrease from  $33^{\circ}\text{C}$  to  $25^{\circ}\text{C}$ . Modeled compress mid-plane temperatures comprise the standard deviation of experiment. However, the shape of both graphs is slightly different. In the simulation, the compress is cooled slower than in the experiment; therefore, the mid-plane temperature of compress after 15 s is lower in the simulation. Small difference in temperature is noticed for different thermoregulation approaches. For the passive thermoregulation model, temperature is marginally higher than for the active thermoregulation model because vasoconstriction provides additional insulation for the tissue.

Figure 8 shows the CFD simulation result for both the passive and the active thermoregulation compared to the mean  $\pm$ SD of  $N = 8$  recorded total heat flux history samples (for compress-skin interface). For the first five seconds (the highest heat fluxes), a good model agreement with the measured data is observed. Then, the modeled total heat flux is higher than the measured. Because of the insulation provided by the vasoconstriction term for the passive thermoregulation, the total heat flux is slightly higher than in the active thermoregulation.

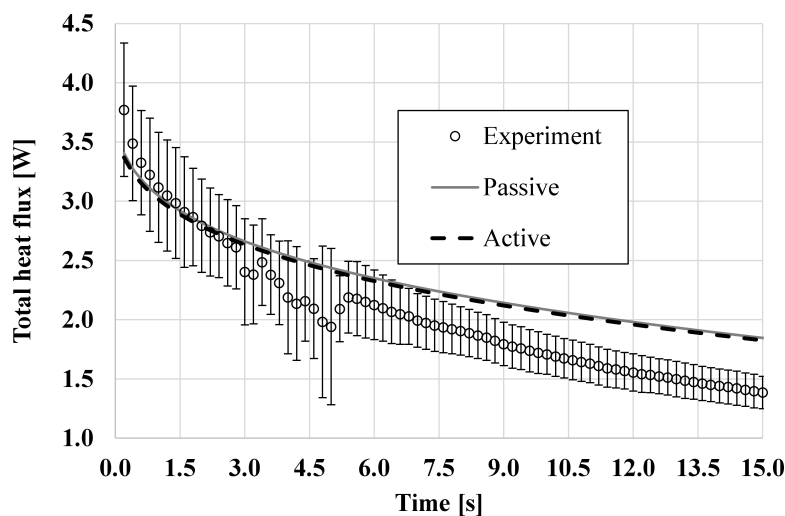


**Fig. 8.** Total heat flux (in W) on compress/skin interface vs. time (s) for experiment (mean  $\pm$ SD,  $N = 8$  samples) and CFD simulation for both passive and active thermoregulation models.

## 5. SUMMARY

As a result of this research, the numerical model of the human forearm undergoing the skin thermostimulation was developed and validated. The vasoconstriction model delivers additional insulation for tissue. Qualitative comparison of the simulation results and the experimental data shows good agreement. The tendency of heat flux and the temperature of the compress are the same for both measurements and computations. According to the obtained results, real-life tissue reveals better insulation properties than in the proposed models. In future research, the measurements on large group of subjects and sensitivity analysis of tissue properties will be performed.

## ACKNOWLEDGMENTS

The work was supported by The National Centre for Research and Development (NCBiR) within project No INNOTECH-K2/IN2/79/182947/NCBR/13 and by Ministry of Science and Higher Education within statutory research funding scheme. This help is gratefully acknowledged herewith.

## REFERENCES

- [1] D. Fiala, K.J. Lomas, M. Stohrer. A computer model of human thermoregulation for a wide range of environmental conditions: the passive system. *J. Appl. Physiol.*, **87**: 1957–1972, 1999.
- [2] D. Fiala, K.J. Lomas, M. Stohrer. Computer prediction of human thermoregulatory and temperature responses to a wide range of environmental conditions. *Int. J. Biometeorol.*, **45**: 143–159, 2001.
- [3] G.W.H. Höhne., W.F. Hemminger, H.-J. Flammersheim. *Differential Scanning Calorimetry*. Springer, 2003.
- [4] Laser Flash Apparatus LFA 457 MicroFlash<sup>®</sup>. Method, Technique Applications of Thermal Diffusivity and Thermal Conductivity.
- [5] Z. Ostrowski, P. Buliński, W. Adamczyk, P. Kozołub, A.J. Nowak. Numerical model of heat transfer in skin lesions. *Zeszyty Naukowe Politechniki Rzeszowskiej, Mechanika*, **87**: 55–62, 2015.
- [6] Z. Ostrowski, P. Buliński, W. Adamczyk, A.J. Nowak, Modelling and validation of transient heat transfer processes in human skin undergoing local cooling. *Przeegląd Elektrotechniczny*, **91**: 76–79, 2015.
- [7] H.H. Pennes. Analysis of tissue and arterial blood temperatures in the resting human forearm. *J. Appl. Physiol.*, **1**: 93–122, 1948.
- [8] N. Severens. *Modelling Hypothermia in Patients Undergoing Surgery*, PhD Thesis. Eindhoven University Press, Eindhoven, 2008.
- [9] N. Severens, W.D. van Marken Lichtenbelt, A.J.H. Frijns, A.A. van Steenhoven, B.A.J.M. de Mol, D.I. Sessler. A model to predict patient temperature during cardiac surgery. *Phys. Med. Biol.*, **52**: 5131–5145, 2007.
- [10] J. Stolwijk. *A Mathematical Model of Physiological Temperature Regulation in Man*. NASA Contractor Report CR-1855, NASA, Washington DC, 1971.
- [11] R. Tadeusiewicz, P. Augustyniak. *Fundamentals of Biomedical Engineering* [in Polish: *Podstawy Inżynierii Biomedycznej. Vol. 1*]. Wydawnictwa AGH, Kraków 2009.